PHYSICAL REVIEW D **89,** 034009 (2014)

Determining the structure of dark-matter couplings at the LHC

Ulrich Haisch,[*] Anthony Hibbs,[†] and Emanuele Re[‡]

Rudolf Peierls Centre for Theoretical Physics, University of Oxford, 1 Keble Road, Oxford OX1 3NP, United Kingdom

(Received 4 December 2013; published 6 February 2014)

The latest LHC monojet searches place stringent bounds on the $pp \to \bar{\chi}\chi$ cross section of dark matter. Further properties such as the dark matter mass or the precise structure of the interactions between dark matter and the standard model, however, cannot be determined in this manner. We point out that measurements of the azimuthal angle correlations between the two jets in $2j + \bar{\chi}\chi$ events may be used to disentangle whether dark matter pair production proceeds dominantly through tree or loop diagrams. Our general observation is illustrated by considering theories in which dark matter interacts predominantly with the top quark. We show explicitly that in this case the jet-jet azimuthal angle difference is a gold-plated observable to probe the Lorentz structure of the couplings of dark matter to top quarks, thus testing the *CP* nature of the particle mediating these interactions.

DOI: 10.1103/PhysRevD.89.034009 PACS numbers: 12.38.Bx, 95.35.+d, 12.38.-t

I. INTRODUCTION

The minimal experimental signature of dark matter (DM) pair production at the LHC would be an excess of events with a single jet in association with large amounts of missing transverse energy ($E_{T,\text{miss}}$). The experimental search for $j + E_{T,\text{miss}}$ events provides bounds on the interaction strength of DM with quarks and gluons, constraining the same parameters as direct detection experiments (see e.g. [1,2]). These measurements place the leading (and in some cases only) limits on models of DM over certain regions of parameter space.

While the $j + E_{T,\text{miss}}$ channel can be used to constrain the $\sigma(pp \to \bar{\chi}\chi)$ cross section, it provides insufficient information to determine additional DM properties such as its mass or the precise nature of its interactions with the standard model (SM). In fact, the transverse momentum (p_T) spectrum of the $j + E_{T,\text{miss}}$ signal is essentially featureless and almost independent of the chirality and/or the *CP* properties of the DM couplings to quarks.[1] This suggests that while ATLAS and CMS are well suited to discover light DM, the LHC prospects of using this channel to make more definitive statements about specific DM properties seem to be slim.

In this paper we observe that this unsatisfactory situation may be remedied by studying two-jet final states involving $E_{T,\text{miss}}$. In particular, we will argue that measurements of the azimuthal angle difference in $2j + E_{T,\text{miss}}$ events can possibly show a strong cosinelike or sinelike correlation only if DM pair production is loop induced, whereas tree-level interactions result in a $\Delta\phi_{j_1 j_2}$ distribution of a quite different shape. In order to illustrate our general observation, we will consider DM models that generate the effective operators

$$\mathcal{O}_S = \frac{m_t}{\Lambda_S^3}\bar{t}t\bar{\chi}\chi, \qquad \mathcal{O}_P = \frac{m_t}{\Lambda_P^3}\bar{t}\gamma_5 t\bar{\chi}\gamma_5\chi. \tag{1}$$

Examples of Feynman diagrams with an insertion of $\mathcal{O}_{S,P}$ that give rise to a $2j + E_{T,\text{miss}}$ signal are displayed in Fig. 1. For this well-motivated case we will explicitly show that the Lorentz structure of the DM top-quark interactions—and consequently the *CP* nature of the mediator inducing (1)—can be disentangled by measuring the normalized $\Delta\varphi_{j_1 j_2}$ distribution. After a discovery of an enhanced monojet signal, combining the measurements of the top-loop-induced $\sigma(pp \to j + \bar{\chi}\chi)$ cross section [4,5] and the $1/\sigma d\sigma(pp \to 2j + \bar{\chi}\chi)/d\Delta\phi_{j_1 j_2}$ spectrum of the jet-jet azimuthal angle difference would allow us to determine not only the suppression scales $\Lambda_{S,P}$ in (1) but also whether the scalar operator $\mathcal{O}_S$ or the pseudoscalar operator $\mathcal{O}_P$ is responsible for the observed excess of $j + E_{T,\text{miss}}$ events. Other constraints on effective interactions between DM and top quarks have been discussed for example in [6,7].

Our work is organized as follows: in Sec. II we introduce the DM interactions which we intend to examine. In Sec. III we calculate the azimuthal angle correlations of the two jets in $2j + \bar{\chi}\chi$ production induced by the operators $\mathcal{O}_{S,P}$, including the full top-quark mass dependence of the squared matrix elements. Our calculation is performed at the leading order (LO) in QCD. We will also comment on the applicability of the heavy top-quark approximation and the impact of higher-order QCD effects. In Sec. IV we

[*]u.haisch1@physics.ox.ac.uk
[†]Anthony.Hibbs@physics.ox.ac.uk
[‡]Emanuele.Re@physics.ox.ac.uk

[1]For instance, the p_T spectra corresponding to effective vector and axial-vector DM-quark interactions are within the uncertainties present at the next-to-leading order (NLO) plus parton-shower (PS) level [3] indistinguishable.

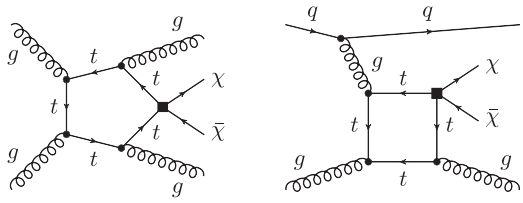

FIG. 1. Typical one-loop diagrams leading to $2j + E_{T,\mathrm{miss}}$ events in pp collisions. The black squares denote insertions of the four-fermion operators $\mathcal{O}_{S,P}$.

discuss the case where the mediator can be resonantly produced, before concluding in Sec. V.

II. DM INTERACTIONS

In the following we are interested in DM pair production from quark or gluon initial states. We will restrict our discussion to the case where the production proceeds via the exchange of a spin-0 s-channel mediator. We consider the following interactions between DM and top quarks involving a colorless scalar (S) or pseudoscalar (P) mediator[2]

$$\mathcal{L}_S = g_\chi^S(\bar{\chi}\chi)S + g_t^S\frac{m_t}{v}(\bar{t}t)S,$$
$$\mathcal{L}_P = ig_\chi^P(\bar{\chi}\gamma_5\chi)P + ig_t^P\frac{m_t}{v}(\bar{t}\gamma_5 t)P, \quad (2)$$

where $v \simeq 246$ GeV is the Higgs vacuum expectation value. Notice that we have assumed that the couplings of the mediators to top quarks are proportional to the associated SM Yukawa coupling. This is motivated by the hypothesis of minimal flavor violation (MFV), which curbs the size of dangerous flavor-changing neutral current processes and automatically leads to a stable DM candidate [8]. While the DM particle χ in (2) is understood to be a Dirac fermion, extending our discussion to Majorana DM or the case of a complex/real scalar is straightforward (see [4] for details).

If the mediator masses $M_{S,P}$ are large compared to the invariant mass $m_{\bar{\chi}\chi}$ of the DM pair, we can describe $2j + \bar{\chi}\chi$ production by means of an effective field theory (EFT). Integrating out the scalar and pseudoscalar mediator then gives rise to (1) as well as composite operators consisting of four top-quark fields, which we do not consider further.[3] In the case of $\mathcal{O}_S$ the suppression scale Λ_S is related to the mediator mass and the fundamental couplings by

$$\Lambda_S = \left(\frac{vM_S^2}{g_\chi^S g_t^S}\right)^{1/3}, \quad (3)$$

and an analogous expression with $S \to P$ holds for $\mathcal{O}_P$.

With the current $j + E_{T,\mathrm{miss}}$ [4] and $\bar{t}t + E_{T,\mathrm{miss}}$ [7] data, one can exclude values of the suppression scale below roughly 150 GeV (170 GeV) in the scalar (pseudoscalar) case for light DM, which is small compared to typical LHC energies. In order to discuss the validity of the EFT approach (see also [10–15]), we will consider in Sec. IV also the simplest ultraviolet (UV) completion, where (1) arises from the full theory (2) after integrating out the fields S and P. We will see that in this case the analysis becomes more model dependent, because the predictions now depend on $g_t^{S,P}$ and $g_\chi^{S,P}$ as well as the masses $M_{S,P}$ and the decay widths $\Gamma_{S,P}$ of the mediators. Apart from these minor complications our general conclusions will however also hold in the case where the s-channel resonances S, P can be directly produced in pp collisions.

III. DM PRODUCTION WITH TWO JETS

In our analysis we consider $2j + E_{T,\mathrm{miss}}$ production at the LHC with $\sqrt{s} = 14$ TeV center-of-mass (CM) energy. We adopt event selection criteria corresponding to the latest CMS monojet search [2].[4] In this search events of more than two jets with pseudorapidity below 4.5 and transverse momentum above 30 GeV are rejected. In order to suppress QCD djet events, CMS puts an angular requirement on the azimuthal distance between the two tagging jets of $\Delta\phi_{j_1 j_2} < 2.5$. Our reference signal region is defined by $|\eta_{j_1}| < 2.4$, $p_{T,j_1} > 110$ GeV and $E_{T,\mathrm{miss}} > 350$ GeV, but we will comment on the sensitivity of the signal on the p_{T,j_1} and $E_{T,\mathrm{miss}}$ cuts. To improve the separation between the azimuthal angle distribution of the SM background and the $2j + E_{T,\mathrm{miss}}$ signal, we also impose a cut of $m_{j_1 j_2} > 600$ GeV on the invariant mass of the dijet system.

The calculation of the azimuthal distance $\Delta\phi_{j_1 j_2}$ of the $2j + E_{T,\mathrm{miss}}$ signal events is performed with the help of GGFLO which is part of VBFNLO [18], modifying the process $pp \to 2j + h(A)$ appropriately. The GGFLO implementation of the $2j + h(A)$ production process is based on the analytical LO results of [19,20] for the scalar Higgs (h) case and of [21] for the pseudoscalar Higgs (A) case. Our simulations utilize MSTW2008LO parton

[2]LHC constraints on the scalar and pseudoscalar DM-quark interactions involving the light flavors $q = u, d, s, c, b$ have been discussed in [3,5].

[3]Unlike the operator $\bar{t}t\bar{t}\gamma_5 t$, which is strongly constrained because it contributes to the electric dipole moment of the neutron [9], the purely scalar or pseudoscalar four-top operators resulting from (2) are experimentally not well bounded. The appearance of the operator $\bar{t}t\bar{t}\gamma_5 t$ can be avoided by taking the spin-0 mediators S, P to be CP eigenstates.

[4]The cuts imposed in the existing ATLAS and CMS analyses will not be suitable for DM searches at the 14 TeV LHC due to triggering limitations [16]. Our work should hence only be considered as a proof of concept. A more realistic study, including NLO corrections, PS effects and hadronization corrections for both the DM signal and the SM backgrounds, will be presented elsewhere [17].

distributions [22] and jets are constructed according to the anti-k_t algorithm [23] with a radius parameter of $R = 0.5$, which corresponds to the value used in the CMS analysis [2].

We start our numerical analysis by showing results obtained for $\Lambda_{S,P} = 150$ GeV, a DM mass of $m_\chi = 50$ GeV, employing the reference cuts described above. Our choice of parameters will be motivated in Sec. IV. The central values of the corresponding $j + E_{T,\mathrm{miss}}$ and $2j + E_{T,\mathrm{miss}}$ signal cross sections are 675 and 204 fb (1119 and 338 fb) for $\mathcal{O}_S$ ($\mathcal{O}_P$), while the SM background predictions amount to 1289 and 330 fb. To put these numbers into perspective we recall that the latest CMS analysis [2] excludes excesses in the monojet cross section with signal-over-background ratios of $S/B \gtrsim 0.15$ at 95% confidence level. Given these numbers the monojet signals corresponding to $\Lambda_{S,P} = 150$ GeV and $m_\chi = 50$ GeV should be easily detectable at the 14 TeV LHC.

The normalized $\Delta\phi_{j_1 j_2}$ distributions associated to the operators $\mathcal{O}_{S,P}$ are displayed in Fig. 2. From the figure it is evident that the scalar operator $\mathcal{O}_S$ produces a strong correlation between the two jets, with a distribution that is peaked at $\Delta\phi_{j_1 j_2} = 0$ and heavily suppressed at $\Delta\phi_{j_1 j_2} = \pi/2$ (red solid curve). In the case of the pseudoscalar operator $\mathcal{O}_P$ the position of the peak and trough is instead reversed (blue solid curve). The cosinelike (sinelike) modulation in the azimuthal angle distribution corresponding to $\mathcal{O}_S$ ($\mathcal{O}_P$) should be contrasted with the spectrum of the dominant SM background process, $pp \to 2j + Z(\to \bar{\nu}\nu)$, which has a minimum at $\Delta\phi_{j_1 j_2} = 0$ and a maximum in the vicinity of $\Delta\phi_{j_1 j_2} = 2.5$ (green solid curve). We simulate the background at LO using the POWHEG BOX [24,25]. PS effects or hadronization corrections are not included in our SM prediction.

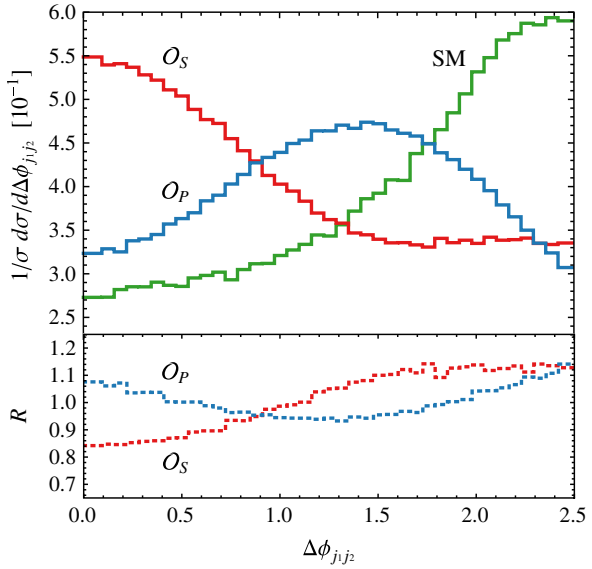

FIG. 2 (color online). Normalized $\Delta\phi_{j_1 j_2}$ distribution for the insertion of $\mathcal{O}_S$ (red) and $\mathcal{O}_P$ (blue) applying the cuts $p_{T,j_1} > 110$ GeV and $E_{T,\mathrm{miss}} > 350$ GeV. The solid curves correspond to the full results while the dotted curves show the ratio R between the results in the heavy top-quark mass approximation and the exact predictions. For comparison the green solid curve indicates the prediction of the dominant SM background process, $pp \to 2j + Z(\to \bar{\nu}\nu)$, using the same event selection criteria. For further details see text.

To assess the significance of our findings, we study the scale uncertainties of the results. As advocated in [20], we identify the factorization scale as $\mu_F = \xi(p_{T,j_1} p_{T,j_2})^{1/2}$ and replace the overall factor α_s^4 entering the $2j + E_{T,\mathrm{miss}}$ cross section by $\alpha_s(\xi p_{T,j_1})\alpha_s(\xi p_{T,j_2})\alpha_s^2(\xi m_{\bar{\chi}\chi})$. We evaluate these quantities for every event generated by our Monte Carlo (MC) and vary ξ in the range $[1/2, 2]$. In the total cross sections the induced scale uncertainties are around $^{+80\%}_{-40\%}$, while the relative shifts in the normalized differential azimuthal angle distributions do not exceed the level of $^{+5\%}_{-5\%}$. We conclude from this that even after considering scale ambiguities, the normalized $\Delta\phi_{j_1 j_2}$ distribution for $\mathcal{O}_S$ is different than that of $\mathcal{O}_P$, and both spectra are clearly distinguishable from the SM background.

The distinction in the radiation pattern of $\mathcal{O}_S$ and $\mathcal{O}_P$ can be most easily understood by employing the heavy top-quark mass limit. In fact, in this approximation the effect of top-quark loops in $2j + E_{T,\mathrm{miss}}$ production can be described in terms of the following two effective operators,

$$\mathcal{O}_G = \frac{\alpha_s}{12\pi\Lambda_S^3} G^a_{\mu\nu} G^{a,\mu\nu} \bar{\chi}\chi,$$
$$\mathcal{O}_{\tilde{G}} = \frac{\alpha_s}{8\pi\Lambda_P^3} G^a_{\mu\nu} \tilde{G}^{a,\mu\nu} \bar{\chi}\gamma_5\chi, \tag{4}$$

where $G^a_{\mu\nu}$ denotes the gluon field strength tensor and $\tilde{G}^{a,\mu\nu} = 1/2\epsilon^{\mu\nu\lambda\rho} G^a_{\lambda\rho}$ its dual.

In the limit that the external partons only experience a small energy loss and that the momentum components of the tagging jets in the beam direction are much greater than those in the transverse plane, the structure of the $pp \to 2j + \bar{\chi}\chi$ matrix element of $\mathcal{O}_G$ and $\mathcal{O}_{\tilde{G}}$ is easy to work out [26]. Denoting the currents and momenta of the gluons that initiate the scattering by $J_{1,2}$ and $q_{1,2}$, one finds in the case of $\mathcal{O}_G$ the result $\mathcal{M}_G \sim J_1^\mu J_2^\nu (g_{\mu\nu} q_1 \cdot q_2 - q_{1\nu} q_{2\mu}) \sim \vec{p}_{T,j_1} \cdot \vec{p}_{T,j_2}$. This implies that the $\Delta\phi_{j_1 j_2}$ spectrum corresponding to $\mathcal{O}_S$ should be enhanced for collinear tagging jets, $\Delta\phi_{j_1 j_2} = 0$, while for $\Delta\phi_{j_1 j_2} = \pi/2$ it should show an approximate zero. In the case of $\mathcal{O}_{\tilde{G}}$ one obtains instead $\mathcal{M}_{\tilde{G}} \sim \epsilon_{\mu\nu\lambda\rho} J_1^\mu J_2^\nu q_1^\lambda q_2^\rho \sim \vec{p}_{T,j_1} \times \vec{p}_{T,j_2}$. It follows that the $\Delta\phi_{j_1 j_2}$ distribution for $\mathcal{O}_P$ should have a dip if the two jets are collinear, $\Delta\phi_{j_1 j_2} = 0$, or back-to-back, $\Delta\phi_{j_1 j_2} = \pi$, as the Levi-Civita tensor forces the result to zero. These features are clearly visible in Fig. 2. The above discussion also implies that in any theory in which one of the loop-induced operators in (4) is generated, the azimuthal angle difference in

$2j + E_{T,\mathrm{miss}}$ events will show a strong cosinelike or sinelike correlation. In theories in which DM pair production proceeds dominantly via tree-level graphs this will not be the case. Measurements of the $\Delta\phi_{j_1 j_2}$ spectrum are thus in principle sensitive to the quantum structure of the DM interactions with the SM.

The lower part of Fig. 2 also shows that while the predictions obtained in the heavy top-quark mass approximation (dotted red and blue curves) describe the full results (solid red and blue curves) within an accuracy of $\pm 20\%$ or better, taking this limit always reduces the amplitude of the cosinelike and sinelike modulations. The behavior found for $1/\sigma d\sigma(pp \to 2j + E_{T,\mathrm{miss}})/d\Delta\phi_{j_1 j_2}$ is in clear contrast to that obtained in the case of the loop-induced monojet cross section for which the limit $m_t \to \infty$ is not a good approximation [4], because the high-p_T jet is able to resolve the sub-structure of the top-quark loop. In fact, also in the case of $\sigma(pp \to 2j + \bar{\chi}\chi)$, we find that the EFT predictions and the exact results are vastly different. For our standard cuts the infinite top-quark mass approximation overestimates the $2j + E_{T,\mathrm{miss}}$ cross section by a factor of around 7 (10) in the case of the operator $\mathcal{O}_S$ ($\mathcal{O}_P$).

In order to further illustrate this point we show in Fig. 3 the normalized $\Delta\phi_{j_1 j_2}$ distributions for $\mathcal{O}_{S,P}$ using again $\Lambda_{S,P} = 150$ GeV and $m_\chi = 50$ GeV, but applying the stronger signal cuts $p_{T,j_1} > 350$ GeV and $E_{T,\mathrm{miss}} > 500$ GeV. The corresponding $j + E_{T,\mathrm{miss}}$ and $2j + E_{T,\mathrm{miss}}$ cross sections read 214 and 87 fb ($\mathcal{O}_S$), 344 and 141 fb ($\mathcal{O}_P$) and 246 and 92 fb (SM). One first observes that the infinite top-quark mass limit still furnishes an acceptable description of the full results in this case. Second, the cosinelike and sinelike modulations of the $\Delta\phi_{j_1 j_2}$ spectra

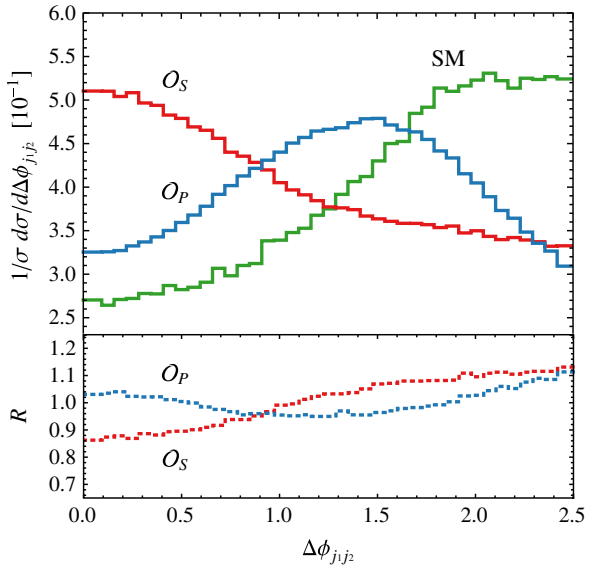

FIG. 3 (color online). Normalized $\Delta\phi_{j_1 j_2}$ distributions using the event selection criteria $p_{T,j_1} > 350$ GeV and $E_{T,\mathrm{miss}} > 500$ GeV. The style and color coding of the curves follows the one used in Fig. 2.

are less pronounced if the requirements on p_{T,j_1} and $E_{T,\mathrm{miss}}$ are more exclusive. This feature can be understood by recalling that a pure cosinelike or sinelike $\Delta\phi_{j_1 j_2}$ spectrum requires that the transverse momenta of the jets are much smaller than the momentum components along the beam direction. For harder p_{T,j_1} cuts this approximation is not as good and as a result the strong jet-jet correlation is less marked. We conclude from this that in order to maximize the power of the $\Delta\phi_{j_1 j_2}$ distribution in determining the Lorentz structure of the DM top-quark interactions the p_{T,j_1} and $E_{T,\mathrm{miss}}$ cuts should be as loose as possible. Making this statement more precise would require to perform a dedicated analysis of the cut dependencies of both the signal and the background. While such a study is beyond the scope of this letter, we plan to return to this question in a future publication [17].

Another important and related issue is the question of whether higher-order QCD effects can potentially wash out the observed strong correlations between the two jets. This question can be addressed by relying again on the similarities of the signal process $pp \to 2j + E_{T,\mathrm{miss}}$ and its QCD analog $pp \to 2j + h(A)$. In the latter case it has been shown by explicit calculations (see e.g. [27–29]) that the shape of the lowest order distributions are unchanged and that therefore the jet-jet correlations survive the addition of NLO QCD corrections as well as PS and hadronization effects. We verified that the latter feature is also present in the case of $1/\sigma d\sigma(pp \to 2j + \bar{\chi}\chi)/d\Delta\phi_{j_1 j_2}$ by showering our LO results with PYTHIA 6.4 [30]. We find that PS effects result in relative shifts of maximal $^{+8\%}_{-8\%}$ in the $\Delta\phi_{j_1 j_2}$ distributions and slightly reduce the amplitudes of the cosinelike and sinelike modulations, but do not distort the spectra. Given its stability under radiative corrections, we believe that the normalized spectrum of the azimuthal angle difference $\Delta\phi_{j_1 j_2}$ in $2j + \bar{\chi}\chi$ production is a gold-plated observable for determining the structure of the couplings of DM to top quarks.

IV. DISCUSSION

Until now we have considered an EFT framework to interpret a hypothetical monojet signal. This is particularly simple because in such a case the complete information is encoded in the scales $\Lambda_{S,P}$ that suppress the effective couplings (1), making it unnecessary to specify details of the particle mediating the interactions. Given the weakness of the bounds on $\Lambda_{S,P}$ [4,7], there are however serious concerns regarding the validity of the EFT approach (see also [10–15] for similar discussions). In this section, we will therefore quantify when the simple-minded limits on the scale of the scalar and pseudoscalar interactions apply and under which circumstances the EFT framework breaks down. In order to go beyond the effective description, one has to specify a concrete UV completion. In the following, we will assume that the full theory is provided by (2), which implies that the effective interactions (1) are generated by

the s-channel exchange of the colorless spin-0 states S, P. We will not discuss the case of t-channel exchange of colored spin-0 mediators, which is interesting in its own right and has been utilized in [31,32] to construct MFV DM models where the relic carries top flavor.

We follow [15] to determine the minimum value of the couplings $(g_\chi^{S,P} g_t^{S,P})^{1/2} = (v M_{P,S}^2/\Lambda_{P,S}^3)^{1/2}$ for which the EFT approach is applicable. First, we derive the limits on the suppression scales $\Lambda_{S,P}$ as a function of the DM mass m_χ. For concreteness, our analysis is based on the most recent monojet search by CMS [2] with an integrated luminosity of 19.5 fb^{-1} at $\sqrt{s} = 8$ TeV, utilizing our standard event selection criteria. Second, we calculate $\sigma(pp \to j + E_{T,\mathrm{miss}})$ in the full theory as a function of both m_χ and $M_{S,P}$. The actual computation of the top-loop induced $j + E_{T,\mathrm{miss}}$ cross sections is performed by means of the MC codes developed in [4,5], which give identical results. For each DM mass, the minimum value of $(g_\chi^{S,P} g_t^{S,P})^{1/2}$ consistent with an EFT description is then found from the requirement that the full theory calculation of $\sigma(pp \to j + E_{T,\mathrm{miss}})$ agrees with the corresponding EFT result to better than 20%. In the whole procedure, we take into account that $\Lambda_{S,P}$ and $M_{S,P}$ are related via (3).

The minimal coupling strengths determined in this manner are indicated by the red solid curves and bands in Fig. 4. The width of the bands reflects the dependence of the predictions on the relative width of the mediators, which we vary in the range $\Gamma_{S,P}/M_{S,P} \in [1/(8\pi), 1/3]$ to obtain the shown results. We see that for the EFT to work the couplings of the s-channel mediators to DM and top quarks have to be strong and that increasingly larger values of $(g_\chi^{S,P} g_t^{S,P})^{1/2}$ are needed for an accurate description, if the DM mass lies at or above the weak scale. In fact, in the case of $\mathcal{O}_S$ ($\mathcal{O}_P$) the theory becomes necessarily nonperturbative for $m_\chi \gtrsim 490$ GeV ($m_\chi \gtrsim 580$ GeV) as indicated by the blue dashed curves in the plots. It is important to realize that the values $M_{S,P}$ for which the EFT is applicable are below a TeV if DM is light. To give an example, for $m_\chi = 50$ GeV the displayed EFT limits correspond to $M_S \simeq 370$ GeV and $M_P \simeq 310$ GeV, respectively, if one assumes that the relative widths are $\Gamma_{S,P}/M_{S,P} = 1/3$.

The DM relic abundance also depends on the couplings $g_{\chi,t}^{S,P}$ and the masses $M_{S,P}$. However, this observable is sensitive to the full particle content of the underlying UV theory, because the mass spectrum determines the number and the strengths of the DM annihilation channels. This feature makes the prediction for $\Omega_\chi h^2$ more model dependent than the monojet cross sections analyzed above. For simplicity, we will assume that the couplings and the particle content are completely specified by (2), meaning that only annihilation processes with top quarks and gluon pairs in the final state are possible. We also allow for either scalar or pseudoscalar interactions but not both.

Using the relevant formulas for the annihilation cross sections given in [4] and requiring that the relic abundance saturates the observed value $\Omega_\chi h^2 = 0.119$ [33], we find the green dotted curves in the panels of Fig. 4. The parameter regions to the left and right of the curves correspond to DM overproduction and underproduction in the early universe. From the intersections of the nonperturbativity bounds and the relic density constraints, we obtain the following limit $m_\chi \gtrsim 40$ GeV ($m_\chi \gtrsim 10$ GeV) in the case of the operator $\mathcal{O}_S$ ($\mathcal{O}_P$). Combining all constraints we then find the yellow colored wedges, which correspond to strongly-coupled theories with weak scale DM masses. Numerically, we arrive at $(g_\chi^S g_t^S)^{1/2} \in [3.9, 4\pi]$ and

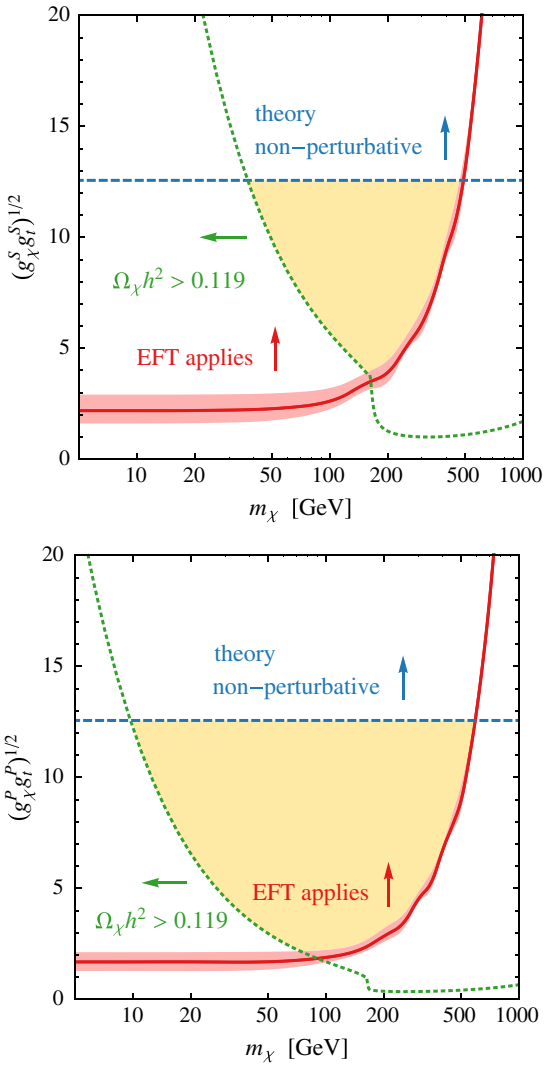

FIG. 4 (color online). Upper panel: The red solid curve and band indicates the minimum value of $(g_\chi^S g_t^S)^{1/2}$ for which the LHC bounds on Λ_S hold. The perturbative limit on this combination of couplings is indicated by the blue dashed curve, while the green dotted curve marks the parameter space where the DM relic density agrees with observation. Lower panel: The analogous bounds on $(g_\chi^P g_t^P)^{1/2}$. In both panels the region of parameter space compatible with all constraints is colored yellow. See text for further explanations.

$m_\chi \in [40, 470]$ GeV $((g_\chi^P g_t^P)^{1/2} \in [2.2, 4\pi]$ and $m_\chi \in [10, 580]$ GeV). The parameters $\Lambda_{S,P} = 150$ GeV and $m_\chi = 50$ GeV used in Sec. III to simulate the $\Delta\phi_{j_1 j_2}$ distributions have hence been specifically chosen so that the EFT approach applies and the universe is not over closed. We emphasize that while large regions of parameter space are excluded due to DM overproduction, these bounds can be ameliorated if DM has large annihilation cross sections to other SM particles or (in particular) new hidden sector states. Such additional annihilation channels can reduce the tension between the LHC monojet limits and the relic density constraints significantly.

The preceding discussion should have made clear that the applicability of the LHC monojet limits on $\Lambda_{S,P}$ is limited. This raises the question of whether the jet-jet azimuthal angle difference in $2j + E_{T,\mathrm{miss}}$ remains a good observable to probe the structure of the DM top-quark interactions also beyond the EFT framework. To answer this question we study a simplified s-channel model described by (2), fixing the relevant parameters to $g_{\chi,t}^{S,P} = 1$, $M_{S,P} = 500$ GeV and $m_\chi = 200$ GeV. Notice that for these parameter choices the DM relic constraints are satisfied. We furthermore verified that our DM models do not lead to an observable signal in existing and future LHC resonance searches in $\bar{t}t$ (dijet) final states. Numerically, we find that including the one-loop process $gg \to S$, $P \to \bar{t}t$ changes the total $\bar{t}t$ cross section by $\mathcal{O}(1\%)$. A dijet signal arises in the simplified models (2) first via the two-loop amplitude $gg \to S$, $P \to gg$, which renders the contributions of S, P exchange to dijet production utterly small.

The signal strength in $j + E_{T,\mathrm{miss}}$ production depends sensitively also on the total widths $\Gamma_{S,P}$ of the mediators S, P. In the case of the scalar mediator, we obtain the following results for the partial decay widths,

$$\Gamma(S \to \bar{t}t) = \left(\frac{m_t}{v} g_t^S\right)^2 \frac{3}{8\pi} M_S \left(1 - \frac{4m_t^2}{M_S^2}\right)^{3/2},$$
$$\Gamma(S \to \bar{\chi}\chi) = (g_\chi^S)^2 \frac{1}{8\pi} M_S \left(1 - \frac{4m_\chi^2}{M_S^2}\right)^{3/2},$$
$$\Gamma(S \to gg) = \left(\frac{m_t}{v} g_t^S\right)^2 \frac{\alpha_s^2}{2\pi^3} \frac{m_t^2}{M_S} \left| F_S\left(\frac{4m_t^2}{M_S^2}\right)\right|^2, \quad (5)$$

where

$$F_S(\tau) = 1 + (1 - \tau)\arctan^2\left(\frac{1}{\sqrt{\tau - 1}}\right). \quad (6)$$

The analog expressions for the pseudoscalar mediator are obtained from (5) by the replacements $S \to P$ and $3/2 \to 1/2$ in the exponents, and the relevant form factor reads

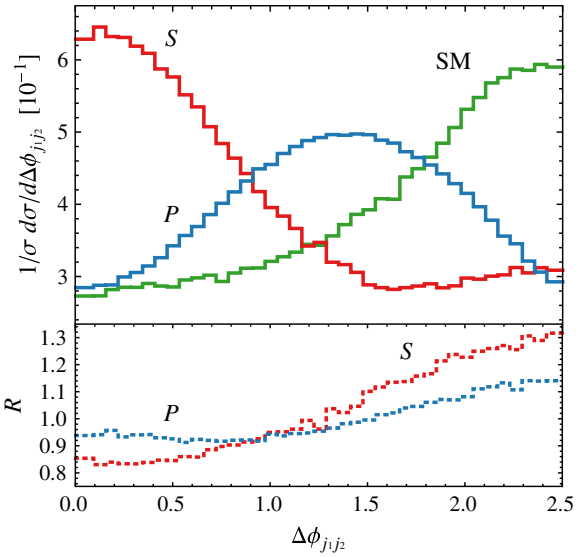

FIG. 5 (color online). Normalized $\Delta\phi_{j_1 j_2}$ distributions arising from a full theory calculation. The used parameters are $g_{\chi,t}^{S,P} = 1$, $M_{S,P} = 500$ GeV and $m_\chi = 200$ GeV and the shown predictions correspond to our reference cuts. The meaning of the colored curves is analogue to the one in Fig. 2.

$$F_P(\tau) = \arctan^2\left(\frac{1}{\sqrt{\tau - 1}}\right). \quad (7)$$

Using the above values for the couplings and masses, we arrive at $\Gamma_S/M_S = 3.1\%$ and $\Gamma_P/M_P = 6.4\%$, which implies that we are dealing with narrow resonances. The corresponding values of the monojet cross sections at the 14 TeV LHC are $\sigma(pp \to j + S(\to \bar{\chi}\chi)) \simeq 9$ fb and $\sigma(pp \to j + P(\to \bar{\chi}\chi)) \simeq 25$ fb, if our standard signal cuts are applied. For the $2j + E_{T,\mathrm{miss}}$ signal cross sections we find instead $\sigma(pp \to 2j + S(\to \bar{\chi}\chi)) \simeq 5$ fb and $\sigma(pp \to 2j + P(\to \bar{\chi}\chi)) \simeq 16$ fb, respectively.[5] At the 14 TeV LHC with an integrated luminosity of 300 fb^{-1} one hence expects to see more than 1000 signal events, which should allow for a measurement of the $\Delta\phi_{j_1 j_2}$ distribution in the $2j + E_{T,\mathrm{miss}}$ sample.

In Fig. 5 we show the normalized azimuthal angle distributions corresponding to our explicit DM models. We see that the strong cosinelike (sinelike) correlation between the two tagging jets in $2j + E_{T,\mathrm{miss}}$ survives in the full theory with resonant scalar (pseudoscalar) exchange. This shows that, unlike the monojet cross section, which depends strongly to the exact model realization, the normalized $\Delta\phi_{j_1 j_2}$ distribution is rather insensitive to the precise structure of the underlying theory, and therefore provides a unique way to probe the anatomy of possible couplings between DM and top quarks.

[5]We recall that the dominant SM backgrounds due to $pp \to j + Z(\to \bar{\nu}\nu)$ and $pp \to 2j + Z(\to \bar{\nu}\nu)$ have cross sections of 1289 and 330 fb, respectively.

As in the case of the EFT calculations, we also see from the latter figure that the $m_t \to \infty$ approximations of the $\Delta\phi_{j_1 j_2}$ spectra describe the exact results reasonably well. We furthermore find that the heavy top-quark mass limit describes the total $2j + E_{T,\mathrm{miss}}$ cross sections much better in the full theory than in the EFT framework. Numerically, we obtain for the standard cuts that the ratio of EFT to exact cross sections is around 1.4 for both scalar and pseudoscalar interactions. The observed feature is explained by the fact that in the full theory the $\sigma(pp \to 2j + E_{T,\mathrm{miss}})$ cross section is dominated by invariant masses $m_{\bar{\chi}\chi}$ close to $M_{S,P}$, while in the EFT calculation the momentum transfer to the DM pair can be (and is on average) much larger. The quality of the heavy top-quark mass approximation however degrades rapidly with the amount of off-shellness [4], which explains why for the total cross sections the $m_t \to \infty$ limit works fairly well in the case of the simplified model, while it fails badly in the EFT approach.

V. CONCLUSIONS

While monojet searches provide already stringent constraints on the pair-production cross sections of DM and may lead to a future discovery at the LHC, even the observation of an unambiguous $j + E_{T,\mathrm{miss}}$ signal will not be enough to determine details of the nature of DM such as the mass of the DM candidate or the structure of its couplings to quarks and gluons. This is due to the fact that while the p_T spectrum of the signal is somewhat harder than that of the background, the enhancement of the high-p_T tail is fairly universal, in the sense that it is independent of the type of interactions that lead to the $j + E_{T,\mathrm{miss}}$ events.

In this paper we have pointed out that some of the limitations of the LHC DM searches can be overcome by studying the jet-jet azimuthal angle difference in final states with two jets and a large amount of missing transverse energy. We showed in particular that if the $2j + E_{T,\mathrm{miss}}$ signal arises from Feynman diagrams involving top-quark loops, measurements of the normalized $\Delta\phi_{j_1 j_2}$ distribution would provide a powerful handle to disentangle whether the DM top-quark interactions are of scalar or pseudoscalar type. In contrast to the prediction of the monojet cross section that is highly model dependent, we emphasized that the strong angular correlation between the two tagging jets is present irrespective of whether the calculation is performed in an EFT or in a simplified DM model with scalar and pseudoscalar exchange in the s channel. This feature combined with the stability of the suggested observable under QCD corrections makes $1/\sigma d\sigma(pp \to 2j + \bar{\chi}\chi)/d\Delta\phi_{j_1 j_2}$ a gold-plated observable to determine the Lorentz structure of the DM top-quark couplings and/or to test the CP properties of the associated mediators.

The method outlined in our work is more general as, after a DM discovery through a $j + E_{T,\mathrm{miss}}$ signal at the LHC, it can in principle be used to tell apart whether DM pair production proceeds dominantly via tree or loop graphs. Only in the latter case, measurements of the azimuthal angle difference in $2j + E_{T,\mathrm{miss}}$ events can potentially show a strong cosinelike or sinelike modulation, while tree-level exchange of spin-0 and spin-1 mediators will lead to a distribution with a rather different $\Delta\phi_{j_1 j_2}$ dependence. In the case of discovery, it is hence imperative that ATLAS and CMS study the differential distributions of final states beyond $j + E_{T,\mathrm{miss}}$.

ACKNOWLEDGMENTS

We would like to thank David Berge, Felix Kahlhoefer, Steven Schramm and Giulia Zanderighi for useful discussions and their valuable comments on the manuscript. Helpful correspondence with Francisco Campanario, Barbara Jaeger and Michael Kubocz concerning GGFLO and VBFNLO is acknowledged. The research of A. H. is supported by an STFC Postgraduate Studentship.

[1] ATLAS Collaboration, Report No. ATLAS-CONF-2012-147.
[2] CMS Collaboration, Report No. CMS-PAS-EXO-12-048.
[3] U. Haisch, F. Kahlhoefer, and E. Re, J. High Energy Phys. 12 (**2013**) 007.
[4] U. Haisch, F. Kahlhoefer, and J. Unwin, J. High Energy Phys. 07 (**2013**) 125.
[5] P. J. Fox and C. Williams, Phys. Rev. D **87**, 054030 (2013).
[6] U. Haisch and F. Kahlhoefer, J. Cosmol. Astropart. Phys. 04 (**2013**) 050.
[7] T. Lin, E. W. Kolb, and L.-T. Wang, Phys. Rev. D **88**, 063510 (2013).
[8] B. Batell, J. Pradler, and M. Spannowsky, J. High Energy Phys. 08 (**2011**) 038.
[9] J. Brod, U. Haisch, and J. Zupan, J. High Energy Phys. 11 (**2013**) 180.
[10] P. J. Fox, R. Harnik, J. Kopp, and Y. Tsai, Phys. Rev. D **85**, 056011 (2012).
[11] I. M. Shoemaker and L. Vecchi, Phys. Rev. D **86**, 015023 (2012).
[12] P. J. Fox, R. Harnik, R. Primulando, and C.-T. Yu, Phys. Rev. D **86**, 015010 (2012).
[13] G. Busoni, A. De Simone, E. Morgante, and A. Riotto, Phys. Lett. B **728**, 412 (2014).
[14] S. Profumo, W. Shepherd, and T. Tait, Phys. Rev. D **88**, 056018 (2013).
[15] O. Buchmueller, M. J. Dolan, and C. McCabe, arXiv:1308.6799.

[16] S. Schramm (private communication).
[17] U. Haisch, A. Hibbs, and E. Re (to be published).
[18] K. Arnold, J. Bellm, G. Bozzi, F. Campanario, C. Englert, B. Feigl, J. Frank, T. Figy *et al.*, arXiv:1207.4975.
[19] V. Del Duca, W. Kilgore, C. Oleari, C. Schmidt, and D. Zeppenfeld, Phys. Rev. Lett. **87**, 122001 (2001).
[20] V. Del Duca, W. Kilgore, C. Oleari, C. Schmidt, and D. Zeppenfeld, Nucl. Phys. **B616**, 367 (2001).
[21] F. Campanario, M. Kubocz, and D. Zeppenfeld, Phys. Rev. D **84**, 095025 (2011).
[22] A. D. Martin, W. J. Stirling, R. S. Thorne and G. Watt, Eur. Phys. J. C **63**, 189 (2009).
[23] M. Cacciari, G. P. Salam, and G. Soyez, J. High Energy Phys. 04 (**2008**) 063.
[24] S. Alioli, P. Nason, C. Oleari and E. Re, J. High Energy Phys. 06 (**2010**) 043.
[25] E. Re, J. High Energy Phys. 10 (**2012**) 031.
[26] T. Plehn, D. L. Rainwater, and D. Zeppenfeld, Phys. Rev. Lett. **88**, 051801 (2002).
[27] V. Del Duca, G. Klamke, D. Zeppenfeld, M. L. Mangano, M. Moretti, F. Piccinini, R. Pittau, and A. D. Polosa, J. High Energy Phys. 10 (**2006**) 016.
[28] J. M. Campbell, R. K. Ellis, and G. Zanderighi, J. High Energy Phys. 10 (**2006**) 028.
[29] J. R. Andersen, K. Arnold, and D. Zeppenfeld, J. High Energy Phys. 06 (**2010**) 091.
[30] T. Sjostrand, S. Mrenna, and P. Z. Skands, J. High Energy Phys. 05 (**2006**) 026.
[31] A. Kumar and S. Tulin, Phys. Rev. D **87**, 095006 (2013).
[32] B. Batell, T. Lin, and L.-T. Wang, arXiv:1309.4462.
[33] P. A. R. Ade *et al.* (Planck Collaboration), arXiv:1303.5076.